Available online at www.sciencedirect.com

ScienceDirect

journal homepage: www.elsevier.com/locate/he

Short Communication

Highly H_2 permeable SAPO-34 membranes by steam-assisted conversion seeding

Liang Zhou [a], Jianhua Yang [a,*], Gang Li [b], Jinqu Wang [a,*], Yan Zhang [a], Jinming Lu [a], Dehong Yin [a]

[a] State Key Laboratory of Fine Chemicals, Institute of Adsorption and Inorganic Membrane, Dalian University of Technology, Dalian, Liaoning 116024, China

[b] School of Light Industry & Food Science, South China University of Technology, Guangzhou 510000, China

ARTICLE INFO

Article history:
Received 17 April 2014
Received in revised form
26 June 2014
Accepted 30 June 2014
Available online 2 August 2014

Keywords:
H_2 separation
SAPO-34 zeolite membrane
Steam-assisted conversion

ABSTRACT

An effective steam-assisted conversion (SAC) seeding method was proposed for the growth of a thin and high-quality SAPO-34 membrane on a low-cost and coarse macroporous α-Al_2O_3 tubular support. This seeding technique was composed of depositing the seeds-containing paste on a support and transforming the paste into continuous and compact seed layer by the SAC process. The paste could serve as the binder to prevent small seeds penetrating into the support. With the aid of the perfect seed layer, a high-quality SAPO-34 membrane with the thickness about 4 μm was synthesized by secondary growth. The as-synthesized membrane exhibited a high H_2 permeance of 6.96×10^{-6} mol m^{-2} s^{-1} Pa^{-1} at room temperature, with H_2/CO_2, H_2/N_2, H_2/CH_4, H_2/C_2H_6, H_2/C_3H_8, H_2/n-C_4H_{10} and H_2/i-C_4H_{10} ideal selectivities of 1.83, 7.58, 14.80, 18.24, 26.51, 40.15 and 53.02, respectively.

Introduction

Hydrogen is a clean energy carrier, which is promising to address greenhouse effect and energy shortage issues [1,2]. About 80% of hydrogen is produced from steam reforming of natural gas and therefore, H_2 must be separated from various impurities, such as CO_2, CH_4, H_2O and CO prior to use in a fuel cell [3]. Among hydrogen purification techniques, membrane separation is particularly attractive due to its easy operation, low energy consumption, and cost effectiveness even at low gas volumes [4]. Although H_2 selective polymer membranes have been well-established in a number of industrial applications, they are restricted to low temperature, non-caustic environments and relatively high sensitivity to swelling and compaction [5]. In comparison, inorganic membranes can well address the harsh requirements in hydrogen produced industry, particularly for the supported zeolite membranes which take advantages of their pore size and shape selectivity with inherent superior mechanical, chemical and thermal stability [6].

So far, many zeolite membranes were already prepared for some practical applications [7]. SAPO-34 with pore diameter of 0.38 nm has been studied for various applications, particularly

* *Corresponding authors*. Tel./fax: +86 411 84986147.
E-mail addresses: yjianhua@dlut.edu.cn, youko16@hotmail.com (J. Yang), wjinqu@dlut.edu.cn (J. Wang).
http://dx.doi.org/10.1016/j.ijhydene.2014.06.159

exhibiting an excellent performance for H_2 separation from N_2, CO_2, CH_4 and some C_2, C_3, C_4-hydrocarbons [8]. According to the previous reports, SAPO-34 membranes were mostly synthesized by secondary growth method, because the nucleation site location and density could be controlled better [9]. It is well recognized that the properties of a seed layer including seed size, coverage, thickness and orientation are very important that directly affect the microstructure and the separation performance of a resulting membrane [10]. Nano-sized seeds are usually inclined to give a better control of membranes formation. To avoid nano-seeds penetrating into supports, small pore size supports are always adopted which result in lower permeance and high membrane production cost. That's against the requirements of the commercial H_2 separation application. The use of cheap coarse macroporous tubular supports can reduce the costs while they impose a high risk of forming defects in the resulting membrane that degrade the separation selectivity. Therefore, the seeding method is particularly significant to form a thin and pinhole/defect free seed layer on a cheap coarse macroporous tube that is the key for the formation of a high performance membrane.

Many seeding methods have been reported including dip-coating, rub-coating, brush-coating, vacuum seeding and so on. But these methods hardly led to perfect seed layers on macroporous supports. By dip-coating rubbing dip-coating (DRD) [11] and varying-temperature hot-dip coating (VTHDC) [12] techniques, the high performances silicalite-1 and T membranes were synthesized on macroporous α-Al_2O_3 tubular supports, respectively. But these seeding procedures were relatively complicated. Recently, rubbing-seed-paste seeding was proposed for the achievement of high PV performance NaA membranes on coarse macroporous supports [13]. Subsequently, impermeable nano-ZSM-5 zeolite coatings were prepared by washcoating and dry-gel conversion method [14]. Inspired by these above seeding methods, a sample and reproducible seeding technology namely steam-assisted conversion (SAC) was proposed for the preparation of SAPO-34 membranes. As shown in Fig. 1, SAC seeding is composed of depositing the seeds-containing paste on a support and transforming the paste into a continuous and compact seed layer by SAC. Through this method, a compact, continuous and high-quality SAPO-34 membrane was prepared on low-cost macroporous support with the thickness about 4 μm. The gas permeation properties of the obtained SAPO-34 membrane were examined using single gases of H_2, N_2, CO_2, CH_4, C_2H_6, C_3H_8, n-C_4H_{10} and i-C_4H_{10}. The evolution process of this seeding technique was also investigated in this paper.

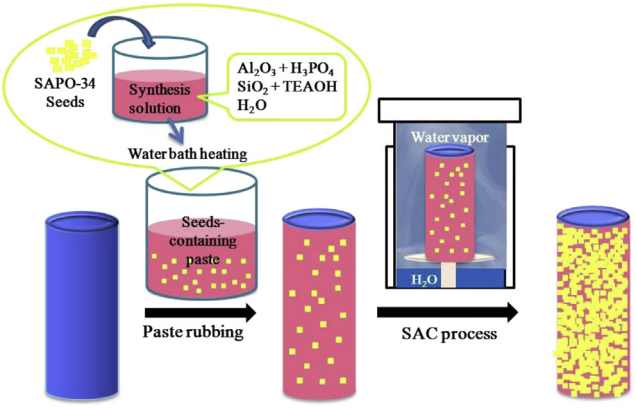

Fig. 1 – Schematic representation of the seed layer formation.

Experimental

Materials

Macroporous α-Al_2O_3 tubes (O.D. 13 mm, I.D. 9 mm and length 50 mm with an average pore size of 2 μm and porosity of 30–40%, Foshan Ceramics Research Institute, China) were used as membrane supports. Ludox AS-40 colloidal silica (40%, Aldrich), Aluminum isopropoxide (AIP, Tian Chemical Agent, China >99.5%) and H_3PO_4 (85wt.% in aqueous, Tian Chemical Agent) were used as silicon, aluminum, phosphorus sources, respectively. Tetraethyl ammonium hydroxid (TEAOH 35wt.%, Hangzhou Yanshan Chemical Agent) and Dipropylamine (DPA, 99%, Aldrich) acted as structure directing agents.

Preparation of the seed layer and membranes

SAPO-34 crystals with an average particle size of 0.5 μm were hydrothermally synthesized according to the previously published procedure [15]. Measured 0.55 g SAPO-34 crystals and mixed uniformly into 37 g synthesis solution with the molar compositions of 1 Al_2O_3:2 P_2O_5:0.6 SiO_2:2 TEA_2O:75H_2O. The overmuch water of the mixture was evaporated at 333 K and then the gelatinous seeds-containing paste was obtained. Before seeding, both ends of the support were sealed by Teflon plugs and the surface of the support was wetted in water. After drying at room temperature, the paste was rubbed onto the outside surface of the support. The coated support was dried at 323 K for 2 h and placed in an autoclave with certain deionized water at the bottom. A continuous seed layer was prepared at 473 K after a 24 h SAC procedure. SAPO-34 membranes were synthesized with the molar gel composition of 1.0 Al_2O_3:1.0 P_2O_5:0.3 SiO_2:1.0 TEAOH:1.6 DPA:77H_2O as previously described [16]. The seeded support was placed vertically into a steel autoclave and immersed into the synthesis solution and then the autoclave was transferred into a preheated oven at 473 K. After crystallization for 24 h, the membrane was washed several times with deionized water until the pH value of water became neutral and then dried overnight at 323 K. Finally, the membrane was calcined in air at 823 K for 8 h to remove the templates with the heating and cooling rate of 1 K/min.

Characterization

The as-prepared seed layer and membrane were characterized by scanning electron microscopy (SEM) using a NOVA NANO SEM 450 (FEI Company) microscope at an acceleration voltage of 20 kV and a working distance of 8–13 mm after gold coating for the samples. X-ray diffraction (XRD) with a Philips Analytical X-ray diffract meter using Cu Kα radiation was used to analyze the crystalline microstructure of the membranes.

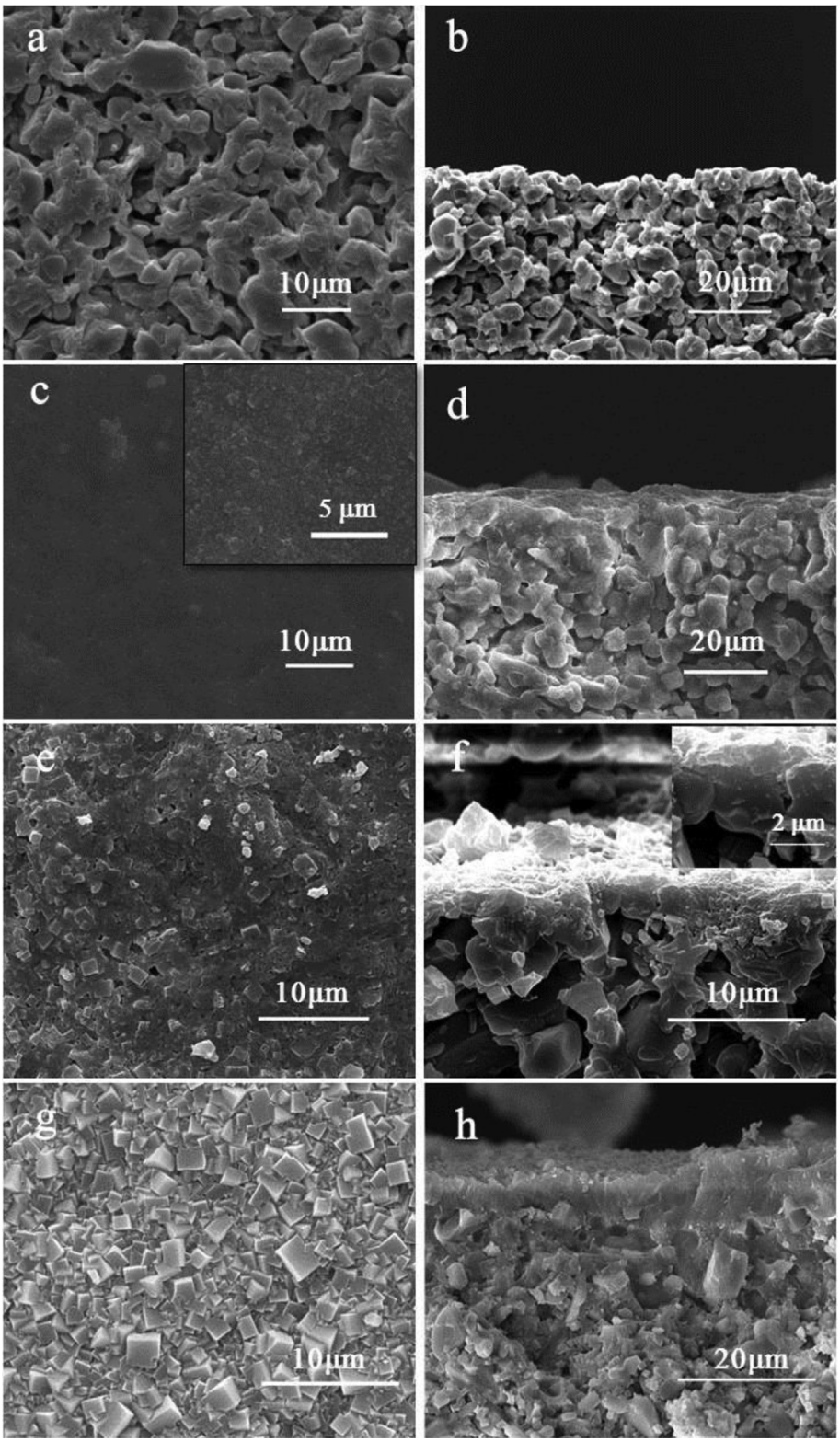

Fig. 2 – Top and cross-section SEM images of the support (a, b), paste layer (c, d), seed layer (e, f) and as-prepared SAPO-34 membrane (g, h).

Gas permeation measurements

Single-gas permeation tests using H_2, CO_2, CH_4, N_2, C_2H_6, C_3H_8, n-C_4H_{10} and i-C_4H_{10} were performed at room temperature and H_2, CO_2, CH_4 and N_2 were tested with the temperature from 298 to 458 K. The pressure drop was 0.1 MPa and the permeate pressure was maintained at atmospheric pressure. The permeate flow rate was determined

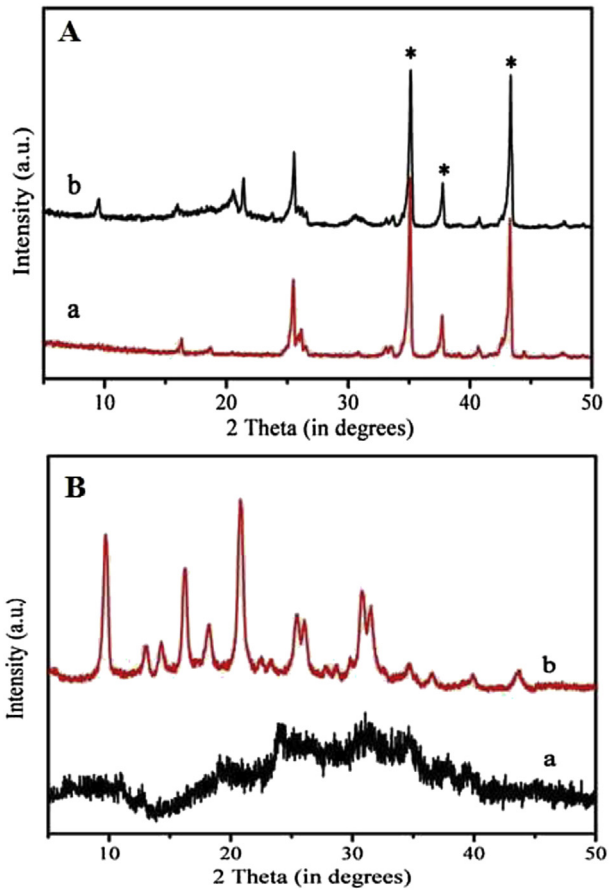

Fig. 3 – XRD patterns of SAPO-34 seed layer by SAC (A-a), as-synthesized SAPO-34 membrane (A-b) on α-Al_2O_3 support, and unsupported seeds-containing paste before (B-a) and after (B-b) SAC.

by a soap-film meter. The permeance P_i for the permeating gas i is defined as follows:

$$P_i = \frac{Q}{A \cdot t \cdot \left(p_f - p_p\right)}$$

where, Q is the moles of gas i permeated through the membrane in a time period of t; A is the total permeation area of the tubular membrane; and p_f and p_p are the partial pressures of the permeating gas in feed side and permeate side, respectively. The permselectivity of $\alpha_{(A/B)}$ is defined as the ratio of permeances of gases A to B.

Results and discussion

A rather rough and discontinuous surface of the original support was obviously seen in Fig. 2a. On the contrary, after coating the paste the pores were almost completely covered by the paste and the surface became smooth and some of the seeds were clearly seen from the higher resolution SEM image in Fig. 2c, although most of them were wrapped by the amorphous paste. As shown in Fig. 2d, it was too thin to distinguish the paste layer clearly from the support. However, a well

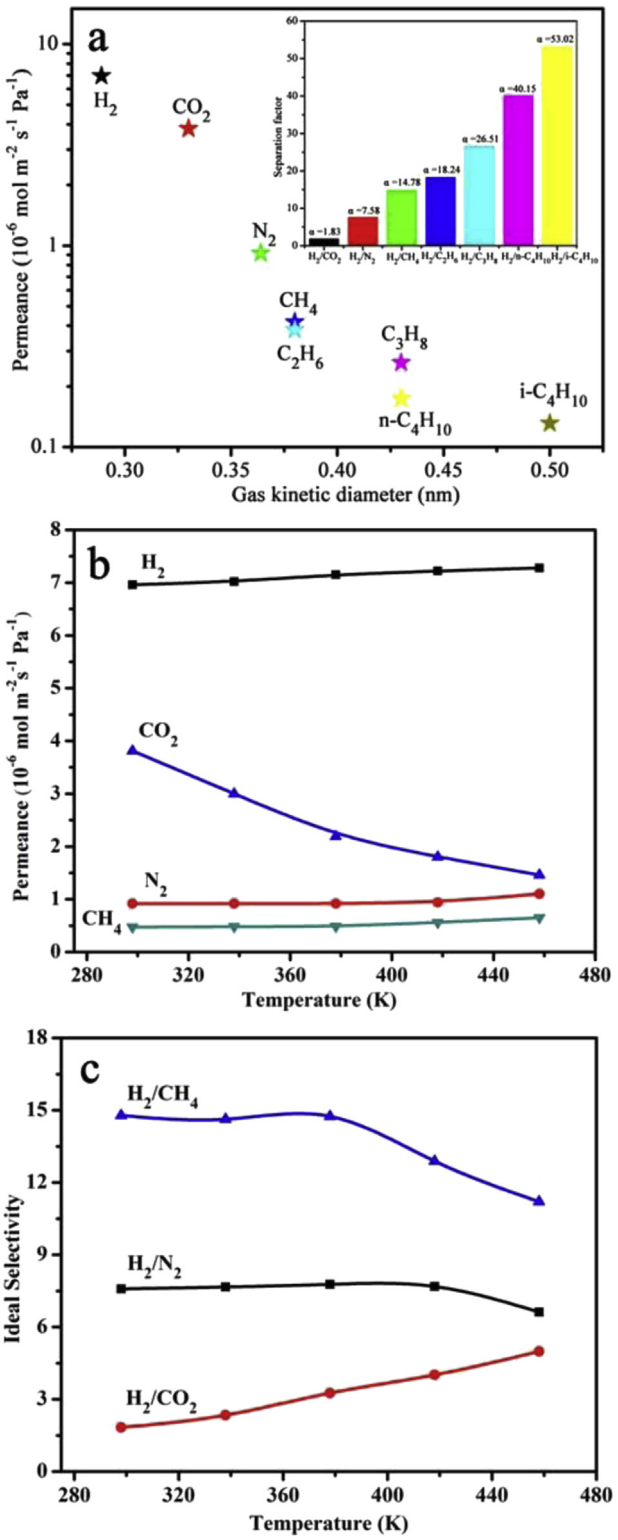

Fig. 4 – Single gas permeances of H_2, N_2, CO_2, CH_4, C_2H_6, C_3H_8, *n*-C_4H_{10} and i-C_4H_{10} and the ideal separation factors for the corresponding gas pairs (a) and their permeances (b) and ideal selectivities (c) for SAPO-34 membrane as a function of temperature with a pressure drop of 0.1 MPa.

Table 1 – Comparison of the gas separation performances of SAPO-34 membrane in this work and with other membranes in the literature.

Membrane/support	Pore size (nm)	Selectivity			H_2 permeances ($mol \cdot m^{-2} s^{-1} Pa^{-1}$)	Separation index π[a]			Ref.
		H_2/N_2	H_2/CH_4	$H_2/i\text{-}C_4H_{10}$		H_2/N_2	H_2/CH_4	$H_2/i\text{-}C_4H_{10}$	
SAPO-34/Clay-Al_2O_3	0.38	20.91	–	–	9×10^{-6}	17.9	–	–	[7]
CHA (AlPO4)/δ-Al_2O_3	0.38	4.1	–	–	7.02×10^{-7}	0.22	–	–	[17]
LTA($AlPO_4$)/α-Al_2O_3	0.4	8.6	8.3	–	1.9×10^{-7}	0.14	0.14	–	[18]
LTA/α-Al_2O_3	0.4	9.4	5.0	–	5.0×10^{-8}	0.042	0.02	–	[19]
LTA (triple-layer)/α-Al_2O_3	0.4	8.6	6.5	–	1.6×10^{-7}	0.12	0.09	–	[20]
NaA/α-Al_2O_3	0.4	4.2	3.6	–	3.0×10^{-7}	0.10	0.08	–	[21]
FAU/α-Al_2O_3	0.74	3.8	2.9	–	1.03×10^{-8}	0.003	0.002	–	[22]
DDR/α-Al_2O_3	0.36	4.75	47.5	–	9.5×10^{-8}	0.036	0.44	–	[23]
Silicate-1/α-Al_2O_3	0.55	1.72	1.23	–	7.9×10^{-6}	0.57	0.18	–	[24]
Silicate-1/S. S. plate	0.55	2.00	2.26	62.86	8.8×10^{-8}	0.088	0.11	5.44	[25]
ZSM-5/Monolith	0.55	2.00	1.04	73	1.6×10^{-7}	0.16	0.006	11.5	[26]
SAPO-34/α-Al_2O_3	0.38	7.58	14.7	53.02	6.96×10^{-6}	4.58	9.54	36.20	This work

[a] $\pi = (H_2 \text{ permeance} \times (\text{selectivity} - 1)) \times \text{permeate pressure}$.

interlocked and compact seed layer with the thickness about 2 μm was observed in Fig. 2f. Moreover, considerable SAPO-34 crystals on the surface were visible from Fig. 2e. As shown in Fig. 2g and h, after secondary hydrothermal growth a compact and well intergrown membrane was formed with no pinholes observed, the thickness of the membrane increased to about 4 μm.

The XRD pattern of the seed layer (as seen in Fig. 3A–a) showed characterization diffraction peaks of SAPO-34 zeolites. The increased crystallinity of the SAPO-34 membrane was confirmed by the higher intensity in Fig. 3A–b. To eliminate the effect of the support, the change during SAC of the unsupported paste was characterized by XRD in Fig. 3B. Because the seeds were covered by the amorphous paste, the crystallinity was rather low. Whereas, the intensities of peaks were increased greatly after SAC and all peaks matched the standard SAPO-34 XRD patterns very well without any other impure phase. The topology of the seed layer is further proved by this unsupported paste conversion, although the intensity is decreased by the support. It is worth noting that the intensity of the XRD patterns of the unsupported seed layer and membrane are quite smaller than the supported seed layer and membrane. That's because the amount of SAPO-34 crystals in them are much lower compared with Al_2O_3 support, therefore, the peaks of Al_2O_3 were much stronger in the membrane, resulting in low relative intensity of SAPO-34 peaks.

The SEM images and XRD patterns show the SAC seeding is benefit to prepare a perfect seed layer and a high-quality SAPO-34 membrane is largely depended on it. There are several advantages of the SAC seeding. The seeds in the paste significantly induce the nucleation and promote the formation of a compact SAPO-34 zeolite layer. Meanwhile, the silica and aluminum precursors in the paste are dissolved by the steam, creating a high saturation degree of the reactants around the SAPO-34 seeds compared with the conventional hydrothermal method. The high saturation degree of the reactants naturally facilitates the growth of SAPO-34 crystals. Furthermore, the paste can serve as a binder to prevent small seeds penetrating into the depth of the support and the resulting intergrown SAPO-34 seeds attach firmly with the support compared with the conventionally deposited separate seeds. Briefly, the SAC seeding provide high density of nucleation sites, high saturation degree of nutrients and high binder strength of the seed layer with the support. Therefore, SAC seeding leads to a high quality SAPO-34 seed layer that has a great significance to the membrane forming.

Fig. 4a shows the permeance of single gas as a function of kinetic diameter at room temperature for SAPO-34 membrane. H_2 had the highest permeance of 6.96×10^{-6} mol $m^{-2} s^{-1} Pa^{-1}$. The permeances were decreased by the increasing of the molecular kinetic diameters. The ideal selectivities for H_2 over light alkanes like CH_4, C_2H_6, C_3H_8 and $n\text{-}C_4H_{10}$ were 14.80, 18.24, 26.51 and 40.15, respectively and that over $i\text{-}C_4H_{10}$ was as high as 53.02. It suggests that these gases follow by the activated diffusion mechanism, except for CO_2. From Fig. 4b and c, the gas permeance of CO_2 was decreased as the temperature increased from 298 to 458 K opposite to H_2, N_2 and CH_4 and so the ideal selectivity of H_2/CO_2 was increased with increasing temperature. The variation of CO_2 follows the surface diffusion mechanism depended on the temperature dependencies of diffusivity and concentration in the activated zeolite pores. At a certain pressure drop, the concentration gradient is small at low temperature where the coverage is nearly saturated. However, the CO_2 coverage may significantly decrease at a high temperature and the increase in diffusivity does not compensate for the decrease in coverage. Thus, the CO_2 permeance was decreased with increasing temperature. As seen in Table 1, the separation indexes of the as-synthesized SAPO-34 membrane were advantageous over most of the reported zeolite membranes for H_2 separation. The remarkably high H_2 permeance is due to the thin and compact SAPO-34 membrane layer. Another important attribution comes from the intrinsic nature of the macroporous support and that reduces the mass transfer resistance. In general, the SAPO-34 membrane prepared by SAC seeding displays a good performance in the hydrogen separation even at high temperature.

Conclusions

A new SAC seeding method was presented for the first time in the fabrication of a high performance SAPO-34 membrane on a low-cost macroporous α-Al_2O_3 support for H_2 separation.

This membrane showed an extremely high H_2 permeance, with the moderate H_2 selectivities over CO_2, N_2, CH_4, C_2H_6, C_3H_8, n-C_4H_{10} and i-C_4H_{10}. The separation indexes were advantageous over most of the reported zeolite membranes for H_2 separation. That's mostly contributed to SAC seeding, which overcame the difficulty in depositing small seeds on a macroporous support and was favored to form a thin and compact membrane. It provided a large possibility and potential for a wide application. Moreover, using of macroporous supports largely promoted the permeance and reduced the cost of the membranes. This method attempts to synthesize highly permeable and affordable SAPO-34 membranes for hydrogen purification. It is believed that the SAC seeding could be extended to other zeolite membranes for improved membrane performances.

Acknowledgments

We are grateful to the financial support from National Natural Science Foundation of China (No. 21076029) and Program for New Century Excellent Talents in University (NCET-10-0286) and National University Student Innovation Program (No. 201110141038).

REFERENCES

[1] Rosen MA, Scott DS. Comparative efficiency assessment for a range of hydrogen production processes. Int J Hydrogen Energy 1998;23:653–9.
[2] Adhikari S, Fernando S. Hydrogen membrane separation techniques. Ind Eng Chem Res 2006;45:875–81.
[3] Nenoff TM, Spontak RJ, Aberg CM. Membranes for hydrogen purification: an important step toward a hydrogen-based economy. MRS Bull 2006;31:735–44.
[4] Spillman RW. Economics of gas separation membranes. Chem Eng Prog 1989;85:41–62.
[5] Wang DK, Diniz da Costa JC, Smart S. Development of rapid thermal processing of tubular cobalt oxide silica membranes for gas separations. J Membr Sci 2014;456:192–201.
[6] Ockwig NW, Nenoff TM. Membranes for hydrogen separation. Chem Rev 2007;107:4078–110.
[7] Das JK, Das N, Bandyopadhyay S. Highly oriented improved SAPO-34 membrane on low cost support for hydrogen gas separation. J Mater Chem A 2013;1:4966–73.
[8] Remy T, Saint Remi JC, Singh R, Webley PA, Baron GV, Denayer JF. Adsorption and separation of C1-C8 alcohols on SAPO-34. J Phys Chem C 2011;115:8117–25.
[9] Hang Chau JL, Tellez C, Yeung KL, Ho K. The role of surface chemistry in zeolite membrane formation. J Membr Sci 2000;164:257–75.
[10] Jabbari Z, Fatemi S, Davoodpour M. Improvement of SAPO-34 fine layer formation on ceramic and steel supports by applying uniform-size synthesized seed particles. Asia-Pac J Chem Eng 2013;8:301–10.
[11] Xiao W, Chen Z, Zhou L, Yang J, Lu J, Wang J. A simple seeding method for MFI zeolite membrane synthesis on macroporous support by microwave heating. Micropor Mesopor Mater 2011;142:154–60.
[12] Chen X, Wang J, Yin D, Yang J, Lu J, Zhang Y, et al. High-performance zeolite T membrane for dehydration of organics by a new varying temperature hot-dip coating method. AlChE J 2013;59:936–47.
[13] Wang Z, Ge Q, Gao J, Shao J, Liu C, Yan Y. High-performance zeolite membranes on inexpensive large-pore supports: highly reproducible synthesis using a seed paste. ChemSusChem 2011;4:1570–3.
[14] You Z, Liu G, Wang L, Zhang X. Binderless nano-HZSM-5 zeolite coatings prepared through combining washcoating and dry-gel conversion (DGC) methods. Micropor Mesopor Mater 2013;170:235–42.
[15] Van Heyden H, Mintova S, Bein T. Nanosized SAPO-34 synthesized from colloidal solutions. Chem Mater 2008;20:2956–63.
[16] Carreon MA, Li S, Falconer JL, Noble RD. SAPO-34 seeds and membranes prepared using multiple structure directing agents. Adv Mater 2008;20:729–32.
[17] Li K, Tian Z, Li X, Xu R, Xu Y, Wang L, et al. Ionothermal synthesis of aluminophosphate molecular sieve membranes through substrate surface conversion. Angew Chem Int Ed 2012;51:1–5.
[18] Huang A, Caro J. Highly oriented, neutral and cation-free AlPO4 LTA: from a seed crystal monolayer to a molecular sieve membrane. Chem Commun 2011;47:4201–3.
[19] Aoki K, Kusakabe K, Morooka S. Gas permeation properties of A-type zeolite membrane formed on porous substrate by hydrothermal synthesis. J Membr Sci 1998;141:197–205.
[20] Huang A, Wang N, Caro J. Synthesis of multi-layer zeolite LTA membranes with enhanced gas separation performance by using 3-aminopropyltriethoxysilane as interlayer. Micropor Mesopor Mater 2012;164:294–301.
[21] Huang A, Liang F, Steinbach F, Caro J. Preparation and separation properties of LTA membranes by using 3-aminopropyltriethoxysilane as covalent linker. J Membr Sci 2010;350:5–9.
[22] Weh K, Noack M, Sieber I, Caro J. Permeation of single gases and gas mixtures through faujasite-type molecular sieve membranes. Micropor Mesopor Mater 2002;54:27–36.
[23] Himeno S, Tomita T, Suzuki K, Nakayama K, Yajima K, Yoshida S. Synthesis and permeation properties of a DDR-type zeolite membrane for separation of CO_2/CH_4 gaseous mixtures. Ind Eng Chem Res 2007;46:6989–97.
[24] Algieri C, Bernardo P, Golemme G, Barbieri G, Drioli E. Permeation properties of a thin silicalite-1 (MFI) membrane. J Membr Sci 2003;222:181–90.
[25] Au LTY, Chau JLH, Ariso CT, Yeung KL. Reparation of supported Sil-1, TS-1 and VS-1 membranes effects of Ti and V metal ions on the membrane synthesis and permeation properties. J Membr Sci 2001;183:269–91.
[26] Kalipcilar H, Gade SK, Noble RD, Falconer JL. Synthesis and separation properties of B-ZSM-5 zeolite membranes on monolith supports. J Membr Sci 2002;210:113–27.